ERDC/CRREL TR-02-15

Cold Regions Research and Engineering Laboratory

US Army Corps of Engineers®
Engineer Research and Development Center

Wide-Area Ice Detection Using Time Domain Reflectometry

Norbert E. Yankielun, Charles C. Ryerson, and Sarah L. Jones October 2002

Abstract: Ice accretion on the wings of fixed-wing aircraft and on the rotors of rotary-wing aircraft can have disastrous results. The ice that forms on a wing structure, especially along the leading edge, modifies the wing aerodynamics, resulting in decreased lift. In the extreme, this can lead to stall and loss of control of the aircraft and potentially a crash. Ice building up elsewhere on the wing, rotor, or airframe can add weight to the aircraft. Several techniques and flight protocols have been developed and are widely used to prevent aircraft from becoming ice covered, both in flight and on the ground.

COVER: Soldiers from D Company, 5th Battalion, 158th Aviation Regiment, clear snow from their Black Hawk helicopter after inclement weather forced an unscheduled stop in Garmisch-Partenkirchen, Germany. The aviators were enroute to the Austrian Alps to help rescue tourists stranded by avalanches. U.S. Army photo by Troy Darr.

How to get copies of ERDC technical publications:

Department of Defense personnel and contractors may order reports through the Defense Technical Information Center:

DTIC-BR SUITE 0944
8725 JOHN J KINGMAN RD
FT BELVOIR VA 22060-6218
Telephone (800) 225-3842
E-mail help@dtic.mil
msorders@dtic.mil
WWW http://www.dtic.mil/

All others may order reports through the National Technical Information Service:

NTIS
5285 PORT ROYAL RD
SPRINGFIELD VA 22161
Telephone (703) 487-4650
(703) 487-4639 (TDD for the hearing-impaired)
E-mail orders@ntis.fedworld.gov
WWW http://www.ntis.gov/index.html

For information on all aspects of the Engineer Research and Development Center, visit our World Wide Web site:

http://www.erdc.usace.army.mil

Technical Report
ERDC/CRREL TR-02-15

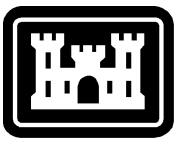

US Army Corps
of Engineers®
Engineer Research and
Development Center

Wide-Area Ice Detection Using Time Domain Reflectometry

Norbert E. Yankielun, Charles C. Ryerson, and Sarah L. Jones

October 2002

Prepared for
OFFICE OF THE CHIEF OF ENGINEERS

PREFACE

This report was prepared by Dr. Norbert E. Yankielun, Geophysical Radar and Electronics Engineer, Engineering Resources Branch, U.S. Army Engineer Research and Development Center (ERDC), Cold Regions Research and Engineering Laboratory (CRREL), Hanover, New Hampshire; Dr. Charles C. Ryerson, Research Physical Scientist, Snow and Ice Branch, ERDC–CRREL; and Sarah L. Jones, Women in Science Program (WISP) Intern, Dartmouth College, Hanover, New Hampshire.

Funding for this research was provided by AT 24, PE 61102, Icing Program, NS004, *Time Domain Reflectometry Wide-Area Ice Detection*.

The authors thank Octagon Process, Inc., for supplying samples of Octaflo EF Type 1 Deicing Fluid and Max Flight Type II and Type IV Anti-Icing Fluid.

CONTENTS

ILLUSTRATIONS

TABLES

Wide-Area Ice Detection Using Time Domain Reflectometry

NORBERT E. YANKIELUN, CHARLES C. RYERSON, AND SARAH L. JONES

1 INTRODUCTION

Ice accretion on the wings of fixed-wing aircraft and on the rotors of rotary-wing aircraft can have disastrous results. The ice that forms on a wing structure, especially along the leading edge, modifies the wing aerodynamics, resulting in decreased lift. In the extreme, this can lead to stall and loss of control of the aircraft and potentially a crash (NTSB 1996, 1997). Ice building up elsewhere on the wing (Fig. 1), rotor (Fig. 2), or airframe can add weight to the aircraft. Several techniques and flight protocols have been developed and are widely used to prevent aircraft from becoming ice covered, both in flight and on the ground.

Figure 1. Cessna 210L covered with snow and glaze ice at Hyde Field, Clinton, Maryland. (Photograph by H. Dean Chamberlain, *FAA Aviation News*, September 2001. Used with permission.)

Figure 2. Military helicopter with ice and snow buildup on rotors and airframe. (Department of Defense photo by Specialist Richard L. Branham, U.S. Army.)

Some, typically larger, aircraft are equipped with in-flight heaters that melt ice before it can substantially build up on wings or rotor blades. Protocols have been established for permitting or denying flight into weather conditions where the potential of aircraft icing is high. On the ground, there are deicing protocols and methods that ensure little to no accretion of ice on wings or rotors immediately prior to flight (Fig. 3) (FAA 1994; Duncan 1995a, b, 1997).

While in flight or on the ground, it is difficult to determine when ice is building up on the aircraft until substantial accretion has taken place. It then may be difficult, or too late, to take evasive maneuvers or rely on the in-flight deicing capability.

On the ground, it would be useful to monitor the state of wing and airframe coverage of deicing fluid, liquid water, or ice. In the air it is useful to detect the presence of ice on the wing, especially runback ice, which forms aft of ice protection areas on the leading edge. This can be a primary cause of control loss. This information can be used to decide when to activate deicing or anti-icing procedures with greater efficiency and economy or when to exit the icing conditions.

Figure 3. Large jet undergoing deicing procedure. (Photo by TSgt Lance Cheung.)

Current icing detectors are single point ice accretion detectors. They are not useful for determining a wide-area spatial distribution of ice, snow, liquid water, or deicing fluids on airframe members (SAE 1995, 2001). They are located to provide a worst-case surrogate for an uninstrumented portion of the aircraft.

We performed preliminary laboratory experiments to explore the use of time domain reflectometry (TDR) and frequency modulated–continuous wave (FM–CW) reflectometry techniques (patents pending) to provide a continuous indication of the presence or absence of liquid water, solid ice, or mixed phase liquid water and ice over large areas of the airframe. We also observe the interface boundaries between ice and glycol-based deicing and anti-icing solutions.

Time domain reflectometry theory

There are at least two functionally different methods for performing the reflectometry for wide-area icing detection: time domain reflectometry (TDR) and frequency modulated–continuous wave (FM–CW) reflectometry. To study the viability of this detection technique, a TDR is directly connected to a parallel transmission line appropriately affixed to an airframe, wing, or rotor.

The principle of TDR is widely known, described in the technical literature, and applied to numerous measurements and testing applications. TDR operates

by generating an electromagnetic pulse (or a fast rise time step) and coupling it to a transmission line. That pulse propagates down the transmission line at a fixed and calculable velocity, a function of the speed of light and the electrical and physical characteristics of the transmission line. The pulse will propagate down the transmission line until the end of the line is reached and then will be reflected back to the source. The time, *t*, in seconds that it takes for the pulse to propagate down and back the length of the transmission line is called the round-trip travel time and is calculated as

$$t = 2L/v \tag{1}$$

where

L = length of the parallel metal rod sensor (m)

v = velocity of propagation (m/s).

The propagation velocity can be given as

$$v = c/(\varepsilon^{1/2}) = c/n \tag{2}$$

where

c = velocity of light in free space (3×10^8 m/s)

ε = the relative dielectric constant of the media surrounding the transmission line

n = index of refraction of the media surrounding the transmission line.

For a two-wire parallel transmission line, changes in the dielectric constant, ε, of the media in the immediate surrounding volume will cause a change in the round-trip travel time.

At any boundary condition along the transmission line (e.g., air/water and water/ice), a dielectric discontinuity exists. As a pulse traveling down the transmission line from the TDR source encounters these boundary conditions, a portion of pulse energy is reflected back to the source from the boundary. A portion of the energy continues to propagate through the boundary until another boundary or the end of the cable causes all or part of the remaining pulse energy to return along the transmission line toward the source. Measuring the time of flight of the pulse and knowing the dielectric medium through which the pulse is traveling permits calculation of the physical distance from the TDR source to each of the dielectric interface boundaries encountered. In this application, the round-trip travel time may be calibrated to indicate whether the instrumented

airframe member is dry or has the presence of ice, liquid water, or deicing fluid. Figure 4 shows a block diagram for a TDR system.

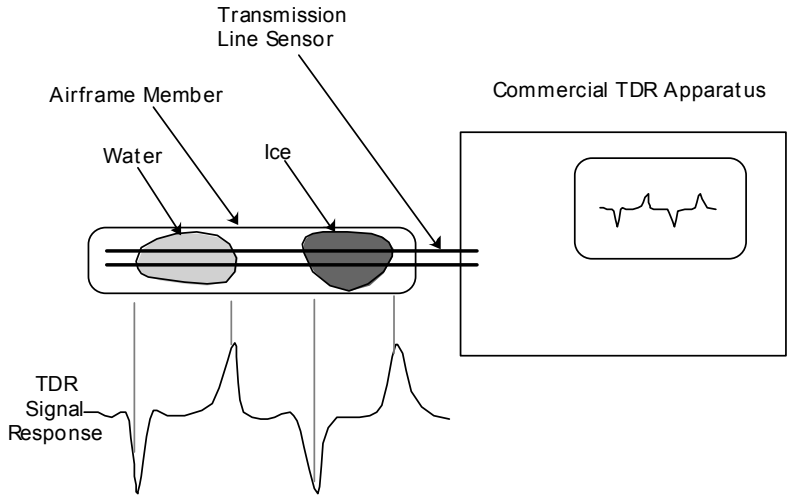

Figure 4. Block diagram of a TDR system.

FM–CW reflectometry theory

A frequency modulated–continuous wave (FM–CW) system can be implemented and applied to the icing problem as an alternative to TDR. FM–CW has been widely used as a radar technique (Skolnick 1980, Botros and Oliver 1986, Botros et al. 1986, Stove 1992, Yankielun et al. 1992) and has proven useful for geophysical applications when coupled with a metallic transmission line (Yankielun 2001).

Here a steady amplitude signal whose frequency increases linearly with time is transmitted down a transmission line. The FM–CW signal is produced by a voltage-controlled oscillator (VCO) driven by a linear ramp generator. This signal, coupled to the transmission line, propagates down the line and is reflected from the far end (or intermediate discontinuity), returning to the source delayed by the round-trip propagation time, $2t_p$. This returning waveform is mixed with a sample of the VCO output that is fed directly to the mixer with a minimal, but known, delay. The mixing process produces sum Σf and difference Δf frequency spectra. Low pass filtering is applied to retain only Δf. Within the bandwidth of Δf , one spectral component, F_D, is proportional to the distance to the end of the parallel transmission sensor, D, and can be determined using spectral analysis

techniques. For a transmission line surrounded by a homogenous dielectric medium with a refractive index n, D is found from

$$D(m) = \frac{(F_D)(t_{swp})c}{2(BW)(n)} \tag{3}$$

where

F_D = difference frequency due to transmission line impedance discontinuity reflection (Hz)

t_{swp} = FM–CW sweep time (s)

c = velocity of light in a vacuum (m/s)

BW = FM–CW swept bandwidth (Hz).

The difference frequency spectra usually lie in the audio range. The spectra can be calibrated as such with distance, D, related to the round-trip travel time, t, by

$$t = (2Dn)/c. \tag{4}$$

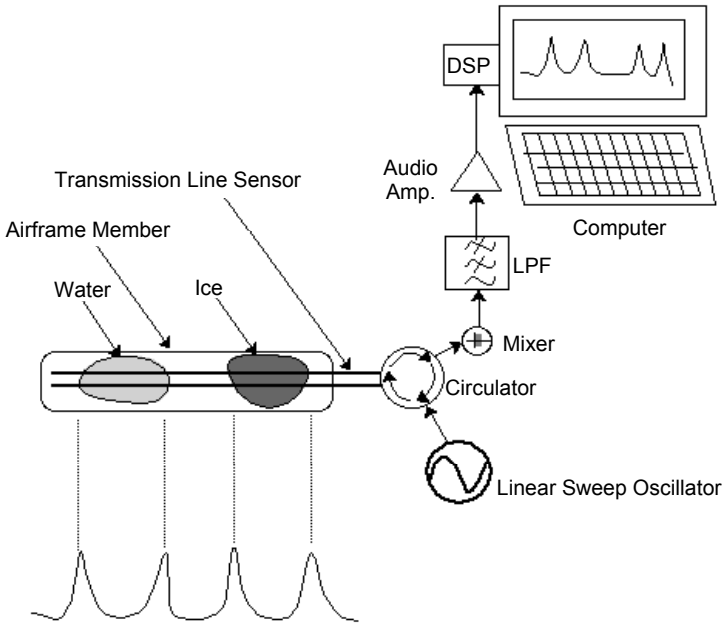

Figure 5. Block diagram of an FM–CW reflectometer.

A typical implementation of an FM–CW transmission line sensor system, as shown in Figure 5, consists of several electronic components. A sweep generator, consisting of a linear ramp generator and voltage controlled oscillator, VCO, is used to create the necessary signal for this implementation. The linear ramp generator is used to periodically drive a rf VCO with sufficient swept bandwidth to provide the required resolution (typically 100 to 1000 MHz of bandwidth). The output of this sweep generator is coupled to the transmission line through a circulator (or T, Magic T, power splitter, or similar device) that permits signal flow from the VCO directly to the transmission line. The swept signal propagates down the transmission line, reaches the distal end, and is reflected back to the circulator. At the circulator, the reflected signal is routed to the mixer diode. There it is mixed with the leakage signal that has propagated across the short path between the VCO and the mixer.

The resulting output of the mixer consists of a high-frequency signal, Σf, and a low-frequency, audio-range difference signal, Δf. The rf low-pass filter (LPF) passes Δf and attenuates Σf to a level making the latter inconsequential. The signal is filtered through an audio high-pass filter (HPF) to remove DC and low-frequency audio components associated with near-end terminal reflections. An audio amplifier may be installed to increase the level of the signal as appropriate for subsequent signal processing. This signal can be directly processed, analyzed, and stored or displayed.

There are several methods by which the resulting audio signal may be processed to provide useful information. It can be viewed directly on an audio-frequency spectrum analyzer where the spectral peaks indicate the dielectric interface boundaries. Using a personal computer with digital signal processing capability, DSP, it can be digitized and processed by an FFT (fast Fourier transform) algorithm, resulting in a power spectrum where the spectral peaks indicate the dielectric interface boundaries.

While the FM–CW system is a viable alternative, it would have to be specifically fabricated for this application. We chose to perform our experiments using a commercially available laboratory-grade TDR system.

Transmission line theory

The characteristic impedance, Z_0, of a parallel transmission line can be calculated by

$$Z_0 = \frac{120}{\sqrt{\varepsilon}} \cosh^{-1}\left(\frac{d}{2a}\right) \tag{5}$$

where

a = radius of the conductors

d = center-to-center distance between the parallel conductors.

We designed the probe to have a $Z_o = 25\ \Omega$ when immersed in water. This impedance will change as the dielectric medium (water or water/ice, ice, water/deicing agent mix) surrounding the sensor changes. However, for our purposes, this change is not problematic.

The dielectric constants, ε, of the materials under consideration are all well known. Fresh water has an $\varepsilon_w = 88$ (at 0°C) and $n_w = 9.4$. Solid, bubble-free, fresh water ice has an $\varepsilon_i = 3.17$ and $n_i = 1.78$ (Ray 1972). There is a wide range of deicing agents (all of proprietary formulation) with an ε_d and n_d that, depending on the solution, are less than that of water. The bulk dielectric constant of a mixture of these components is a function of the dielectric constant of the materials and their volume fractions (Ulaby et al. 1986). Here, for example, a first-order linear mixing formula is used to relate the volume fractions of ice, V_i, and water, V_w, and their respective dielectric constants to estimate the bulk dielectric of the mixture, ε_b:

$$\varepsilon_b = V_w\varepsilon_w + V_i\varepsilon_i = V_w\varepsilon_w + (1 - V_w)\,\varepsilon_i. \tag{6}$$

In the case of an ice/water mix, the bulk dielectric (and consequently the bulk index of refraction) of the mixture will be less than that of liquid water alone. Similar conditions apply for a deicing agent/water mix.

If ice accretes on and around the transmission line, the bulk dielectric constant of the volume immediately surrounding the line decreases and the propagation velocity along the transmission line increases. The sensor round-trip travel time is inversely proportional to the increase in velocity. It is this decrease in round-trip travel time that is measurable by the TDR (or FM–CW reflectometer), and it can be used to indicate the absence, presence, or buildup of ice on the instrumented airframe member.

For a transmission line with two parallel wires, changes in the dielectric media in the immediate surrounding region will cause a change in the velocity of propagation. Baker and Lascano (1989) describe and map this region as an elliptic or quasi-rectangular area surrounding probes submerged in water. By use of the technique described in Knight (1992), the dimension of the region of sensitivity about the parallel transmission line can be estimated for a given cumulative radial energy distribution, $P(\rho, \beta)$, bounded by a region of radius, r, surrounding the parallel transmission line.

$$P(\rho,\beta) = 1 - \frac{\ln\left[\left(\rho^2 + 1 - \beta^2\right)/\left(\rho^2 - 1 + \beta^2\right)\right]}{2\ln\left[\beta^{-1} + \sqrt{\beta^{-2} - 1}\right]}, \rho \geq 1 + \beta \quad (7)$$

where

$\rho = r/d$

$\beta = b/d$

b = radius of the transmission line conductors

d = one-half of the center-to-center distance between the conductors

r = radius of the region of sensitivity around the conductor pair.

2 APPROACH

Glycol concentration and freezing point determination

We prepared solutions of Octaflow (a commercial, Type 1, propylene glycol-based deicing fluid) to concentrations within the manufacturer's specified range for deicing application, and also prepared solutions of MaxFlight (a commercial propylene glycol-based anti-icing fluid) to concentrations within the manufacturer's specified application range. Refractometer measurements of concentration were made and recorded along with the calculated freezing points for glycol/water solutions (Table 1).

Table 1. Prepared deicing and anti-icing solutions by percent volume.*

Product	Volumetric prepared solution	Refractometer measured solution	Freezing point
Deicing (Octaflow)	30%	30%	–9.8°C
"	40%	38%	–14.8°C
"	50%	50%	–21.5°C
"	60%	56%	–30.0°C
Anti-icing (MaxFlight)	50%	50%	–21.5°C
"	75%	67%	–58.0°C
"	100%	100%	> –58.0°C

* Freezing point temperatures are calculated from the refractometer measured solution percentages.

Dielectric constant for glycol deicing and anti-icing solutions

We measured the broadband (100 MHz to 1.3 GHz) complex dielectric (ε' is the real component and ε'' the imaginary) constants of the anti-icing and deicing fluids in their industry-recommended concentrations using a network analyzer and a liquid dielectric test probe. Dielectric measurements were made with an Agilent 8712ET RF Network Analyzer and Agilent 85070B Dielectric Probe Kit and associated dielectric calculating software. This measurement was necessary to confirm that there would be sufficient dielectric contrast at a boundary consisting of deicing fluid (primarily a glycol–water solution) and ice. We also

measured the dielectric of liquid water at room temperature over the same frequency range.

Single-component TDR testing

For homogenous, single solution, or single-phase measurements, we used a 2.44-m-long horizontal trough fabricated from a longitudinally split 7.62-cm-i.d. PVC pipe. The trough was terminated at both ends by a PVC pipe end cap. Two small holes were drilled in each end cap near the bottom of the trough, permitting the insertion of #22 bare, tinned copper wire, forming a transmission line path. The two parallel solid conductor #22 wires were spaced 5 mm apart and 1 mm from the bottom of the trough. Once the wires were inserted through the end caps, the holes were sealed with silicon caulk. One end of the pair wires was connected to screw terminals, permitting connection to a Tektronix 1503C TDR via a 1-m length of RG-58 coaxial cable. The other end of each wire was also connected, under tension, to another pair of screw terminals, electrically terminated as an open circuit (Fig. 6).

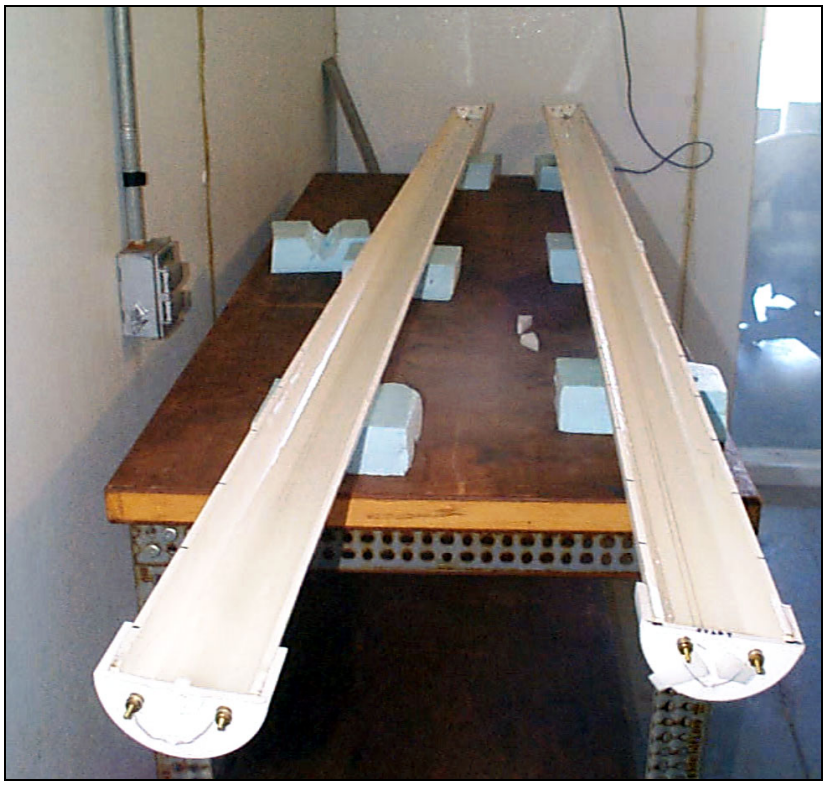

Figure 6. Two troughs in coldroom used for single-component TDR tests.

For all experiments, the TDR was set to generate 2-ns pulses into a 50-Ω load. For noise filtering, the TDR was set to average 16 waveforms. The horizontal scaling of the TDR was set to collect data from the complete length of the test fixture. The TDR data output consisted of a vector of 251 8-bit values representing the reflection waveform. Connection from a serial port on the TDR to a laptop computer enabled acquisition of the waveforms and storage of the data in a spreadsheet format for later analysis. Several single-component tests using the trough were performed (Table 2).

Table 2. Single-component trough tests.

Test	Temperature	Notes
Dry trough	+20°C	Baseline test of apparatus, dry
Water-filled trough	+20°C	Baseline test of apparatus, wet
Water-filled trough	–9.5°C	Monitored freezing process every 15 minutes until fully frozen
Ice-filled trough	+20°C	Monitored thawing process every 15 minutes until fully thawed

Initially, a dry trough was subjected to TDR testing to obtain a set of baseline data. Subsequent testing required the filling of the trough with a sufficient quantity of water, deicing fluid, or anti-icing fluid to slightly cover the entire parallel transmission line sensor. The trough, with water, was placed in a 15°F (–9.5°C) coldroom until it froze. The TDR response was monitored and recorded every 15 minutes during the time required for the fluid to reach ambient temperature and fully freeze (in the case of water). Conversely, the trough was removed from the coldroom and permitted to thaw completely. During that event the TDR response was monitored and recorded every 15 minutes until the trough contained only liquid water.

Two-component TDR testing

For testing of boundary conditions between two states (e.g., frozen and liquid) and two materials (e.g., ice and liquid deicing solution), a vertical tube assembly was fabricated (Fig. 7). This permitted the freezing of water in the lower portion of the tube, clearly defining one component of the boundary condition.

The vertical tube was fabricated from a 5-ft (1.5-m) length of 6.5-mm-thick walled, rigid, clear acrylic tube with an inner diameter of 3.2 cm. Two parallel

uninsulated solid conductor #22 wires were spaced 5 mm apart and located in the center of the acrylic tube. The wires were terminated, under tension, on the top and bottom ends of the tube to screw terminals. The bottom termination was an electrical open circuit. Holes drilled in the bottom end cap of the tube were sealed with silicon caulk. The terminals on the top of the tube permitted connection to a Tektronix 1503C TDR via a 1-m length of RG-58 coaxial cable.

Initially this tube was tested with a single component (e.g., air, water, deicing solution, anti-icing solution) to obtain a baseline set of readings (Table 3). Subsequently, the tube was half-filled with water and permitted to freeze. This provided one component of a boundary condition for interface testing of ice/air, ice/liquid water, and ice/deicing fluid (Table 3), the second component being above the frozen water.

Figure 7. Tube assembly for two-component boundary measurement using TDR.

Table 3. Tube tests with one and two components.

Test	Temperature	Notes
Dry tube	+20°C	Baseline test of apparatus, dry
Water-filled tube	+20°C	Baseline test of apparatus, wet
Water-filled tube	–9.5°C	Monitored freezing process every 15 minutes until fully frozen
Deicing solution (Octaflow)	+20°C	30% by volume solution
"	+20°C	40% by volume solution
"	+20°C	50% by volume solution
"	+20°C	60% by volume solution
"	–9.5°C	30% by volume solution
"	–9.5°C	30% by volume solution
"	–9.5°C	40% by volume solution
"	–9.5°C	50% by volume solution
Anti-icing solution (MaxFlight)	+20°C	50% by volume solution
"	+20°C	75% by volume solution
"	+20°C	100% by volume solution
"	–9.5°C	50% by volume solution
"	–9.5°C	75% by volume solution
"	–9.5°C	100% by volume solution

Wing icing tests using TDR

We performed TDR-based, temperature-regulated, coldroom studies of liquid water/ice/mixed phase/deicing fluid components on an airframe structure, making periodic measurements and observations throughout a complete freezing or thawing cycle of the solutions under test (Table 4). For these tests we used a 3-m section of a composite Black Hawk helicopter blade (Fig. 8). A longitudinal section along the blade was selected for testing. Since the blade has a convex shape, it was necessary to build a barrier that would contain liquid and permit the formation of ice within a confined region surrounding the TDR sensor transmission line wires. The barrier was constructed from strips of self-adhesive closed cell foam placed longitudinally over the Nomex core of the blade, aft of the spar

(Fig. 9). Ice and fluids were separated by a closed-foam dam located in the longitudinal center of the reservoir (Fig. 9). Here, instead of using two bare parallel copper wires for the transmission line, we resorted to the use of a parallel pair of ribbon cable (the type of cable used for computer component interconnection). The wires were approximately 1 mm apart, and the parallel pair was affixed to the wing using a thin layer of flexible rubber adhesive (Fig. 9). The end of the cable was connected to a Tektronix 1503C TDR via a parallel line to BNC adapter and a 1-m-long RG-58 cable.

Table 4. Black Hawk rotor tests.

Test	Temperature	Notes
Dry	+20°C	Baseline test of apparatus, dry
Water	+20°C	Baseline test of apparatus, wet
Ice	–9.5°C	Baseline test of apparatus, frozen
Ice/air	–9.5°C	
Ice/water	–9.5°C	
Ice/deicing (Octaflow)	–9.5°C	30% by volume solution
"	–9.5°C	40% by volume solution
"	–9.5°C	50% by volume solution
"	–9.5°C	60% by volume solution
Ice/anti-icing (MaxFlight)	–9.5°C	50% by volume solution
"	–9.5°C	75% by volume solution
"	–9.5°C	100% by volume solution

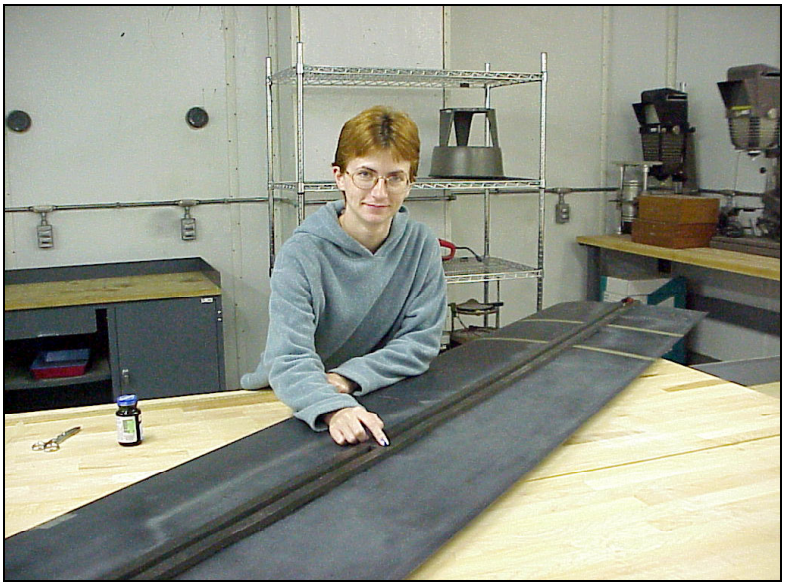

Figure 8. Black Hawk helicopter blade used in icing tests. Finger points to closed foam dam in middle of reservoir.

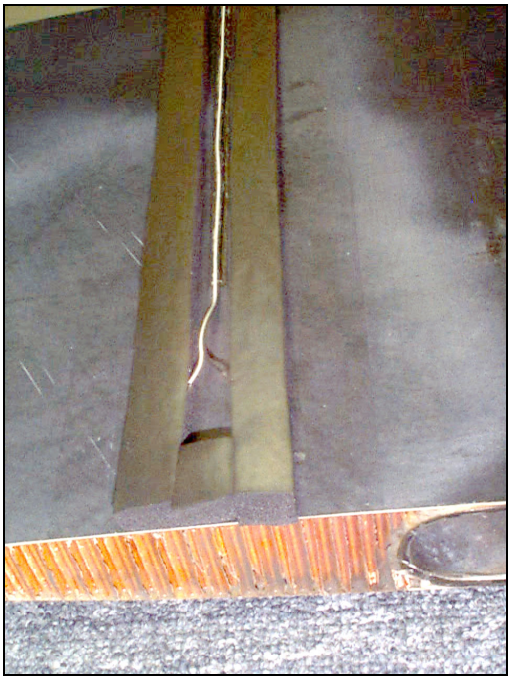

Figure 9. Detail of helicopter blade section showing TDR sensor wiring details. Note location of reservoir over Nomex core of blade aft of spar.

3 RESULTS

Dielectric constant for glycol deicing and anti-icing solutions

Values for the complex dielectric constant of both of the glycol-based solutions were as expected for glycol-based solutions (Fig. 10 and 11). In each test a water sample at 20°C was also tested as a control and for comparison. The water always yielded an ε′ of approximately 80 and a frequency-dependent ε″ in the range of 0 to 5. For both glycol solutions the value of ε′ increased with the increase of the volume fraction of water in the solution, increasing toward the limit of ε′ for water. In all cases the ε″ component of the glycol solutions was substantially greater than that of water; the greater the volume fraction of water in the solution, the less the loss.

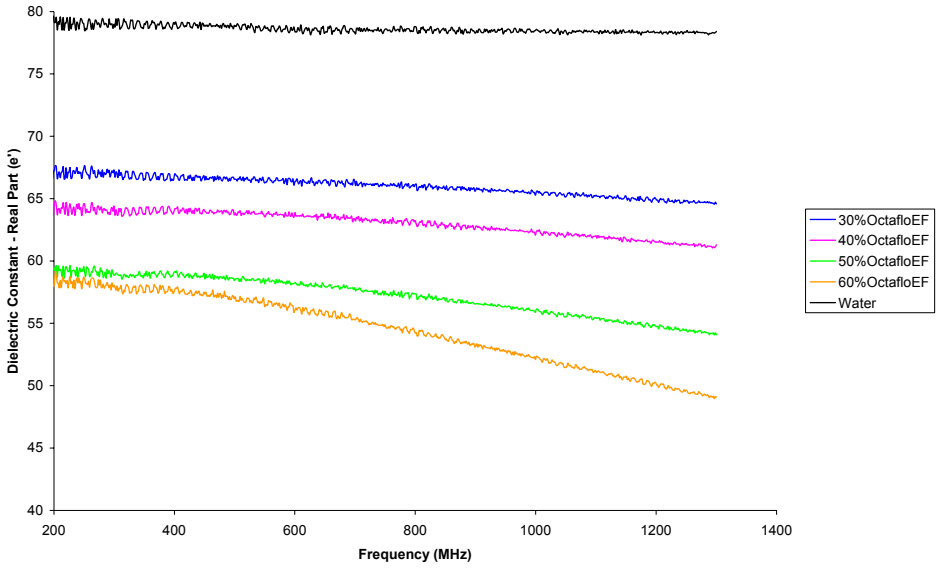

a. Real part, ε′.

Figure 10. Broadband (100 MHz to 1.3 GHz) complex dielectric constant of water and series of glycol-based deicing solutions.

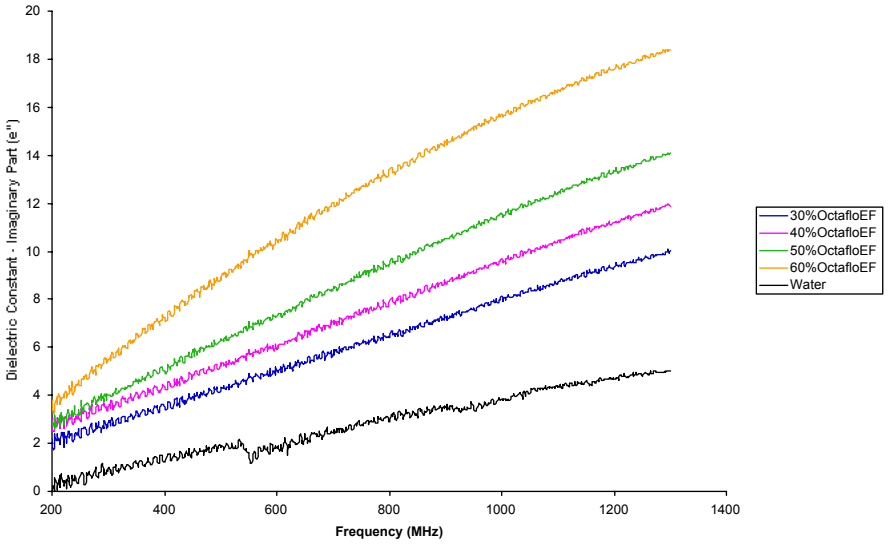

b. Imaginary part ε″.

Figure 10 (cont'd). Broadband (100 MHz to 1.3 GHz) complex dielectric constant of water and series of glycol-based deicing solutions.

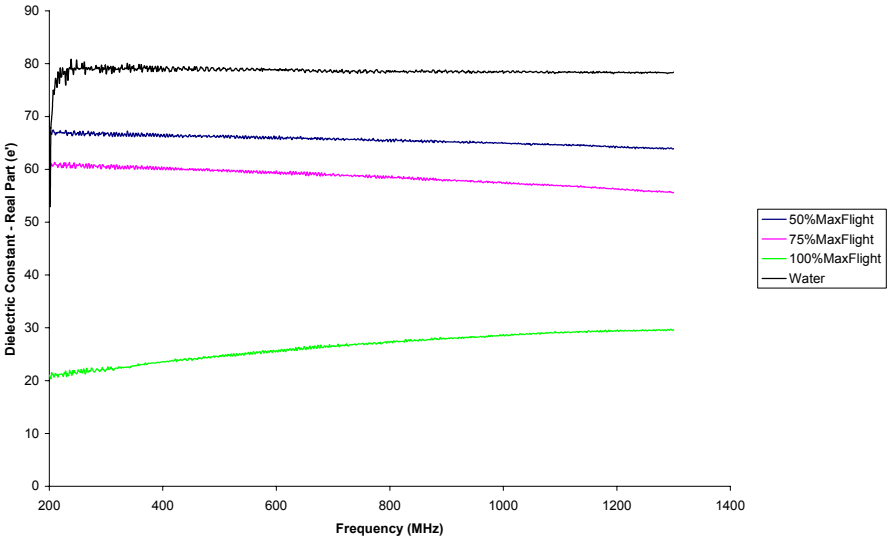

a. Real part, ε′.

Figure 11. Broadband (100 MHz to 1.3 GHz) complex dielectric constant of water and series of glycol-based anti-icing solutions.

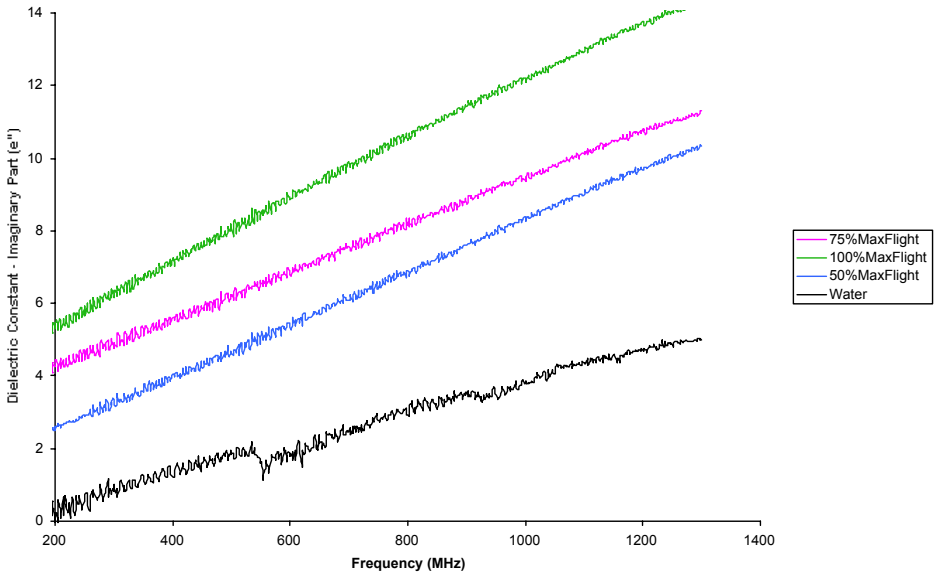

b. Imaginary part ε″.

Figure 11 (cont'd).

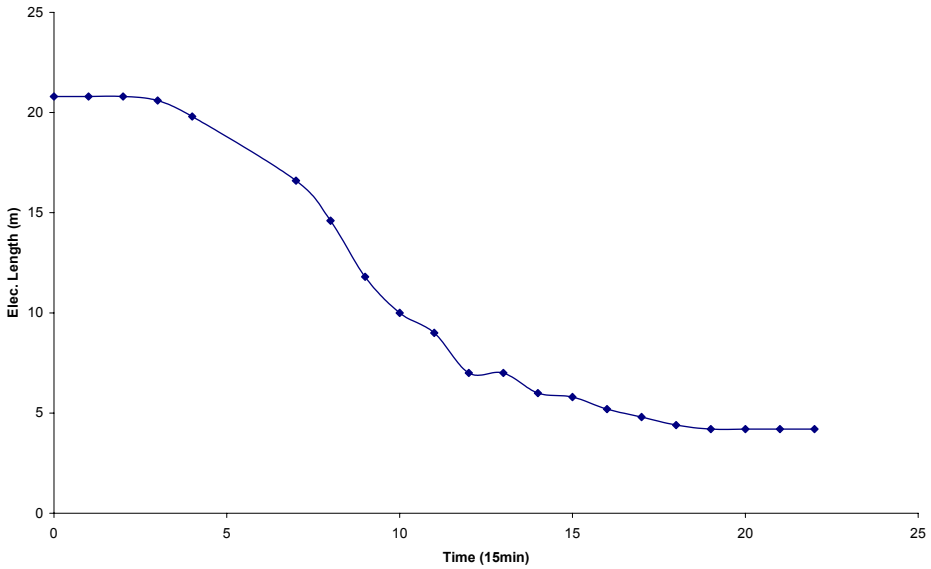

Figure 12. Electrical length of TDR sensor immersed in water while undergoing freezing process.

Single-component TDR testing

These tests were used to confirm that the TDR system would indicate the change in bulk dielectric constant of the contents of the test trough as a state change (i.e., freezing or thawing) occurred. Figure 12 shows the shortening of the electrical length of the trough due to the increasing bulk dielectric constant of the contained water as it froze and changed from an ε′ of 80 to an ε′ of 3.12.

From this changing electrical length and the known parameters of the physical length of the transmission line in the trough, and the dielectric constants for water and ice, the temporal volumetric percent of ice and water distributed in the trough was calculated (Fig. 13).

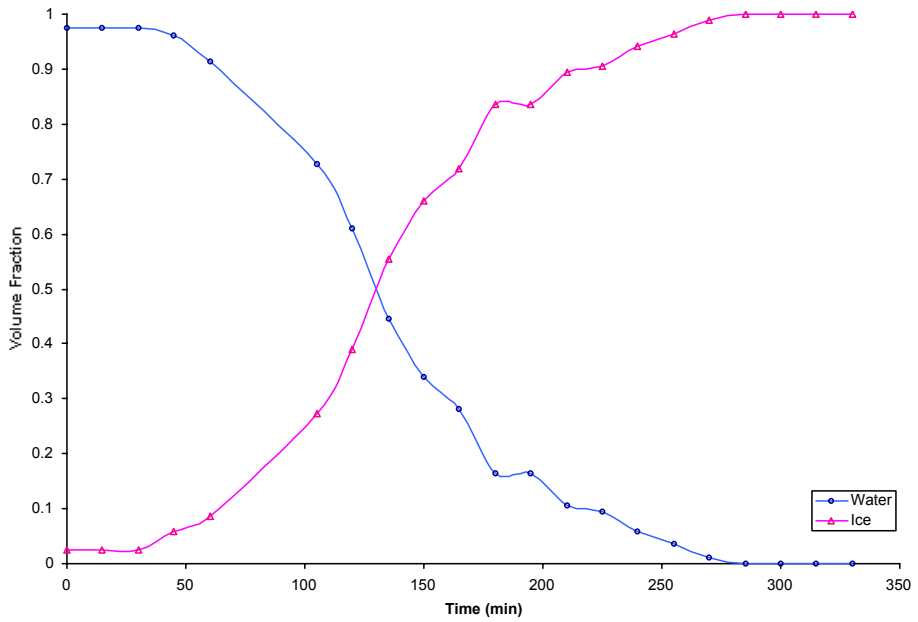

Figure 13. Calculated volume fractions of water and ice during TDR measurements of freezing water.

Two-component TDR testing

Figure 14 shows a comparison of three TDR responses for different two-component interfaces: air/ice, water/ice, and deicing solution/ice in the column. The air/ice TDR waveform shows, from left to right, the start-of-sensor reflection, an air/ice transition, and an end-of-ice reflection pulse. For this case and all subsequent cases, the start-of-sensor reflection pulse is due to the change in

electrical impedance (mismatch) from the 50-Ω coaxial cable to the parallel transmission line sensor. The magnitude of this pulse is a function of the degree of impedance mismatch at this boundary; the greater the mismatch, the greater the pulse magnitude. The next feature of interest in the air/ice waveform is the inflection point indicating the point of the air/ice transition. Instead of seeing a separate reflection pulse, we see here the effect of two spatially close reflection events: the interference of the start-of-sensor pulse with the air/ice reflection pulse. If there were greater physical (or electrical) distance between these adjacent events, two discrete pulses would be apparent.

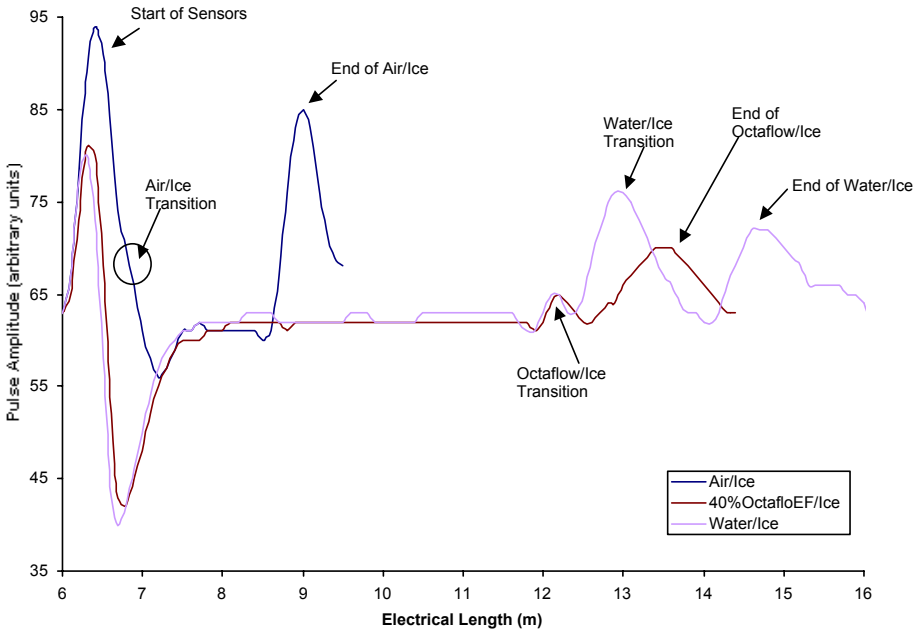

Figure 14. Typical TDR waveforms for several two-component TDR tests. Shown are the waveforms for an air/ice, water/ice, and 40% deicing solution/ice boundaries.

In the case of the water/ice test, shown in Figure 14, from left to right there are three distinct TDR boundary reflection pulses. The first results from the start-of-sensor impedance mismatch boundary. The second is due to the reflection at the water/ice boundary. The third pulse results from end-of-probe reflection. The water/ice boundary reflection pulse is displaced to the right as expected, proportional to the index of reflection of water and the physical distance between the subsequent water/ice boundary. Similarly, the ice-covered section of the probe

between the water/ice boundary and the end-of-sensor pulse for this waveform is consistent with the length of the transmission line embedded in ice.

The third TDR waveform on this graph illustrates a boundary condition between the anti-icing fluid (Octaflow) and ice. Starting from the left, the start-of-sensor waveform is distinct. The transition reflection between the anti-icing solution and the ice is nearly indeterminate as shown in Figure 14 between the two arrows. This indeterminate pulse response is most likely due to the mixing effect resulting at the anti-icing/ice boundary as the anti-icing agent melts the adjacent ice and creates a solution gradient boundary rather than a discrete boundary. A TDR pulse best reflects from a clearly defined, contrasting dielectric boundary. For a boundary that is formed as a gradient (or solution taper) between two contrasting dielectrics, minimal reflection occurs. This condition is analogous to the use of matching networks in electrical circuits to couple two different impedances. The subsequent, and distinct, end-of-sensor reflection pulse is shifted to the left, as compared with the water/ice waveform on the same figure. This result is expected as the 40% by volume anti-icing solution of Octaflow has a lower dielectric constant than that of water alone.

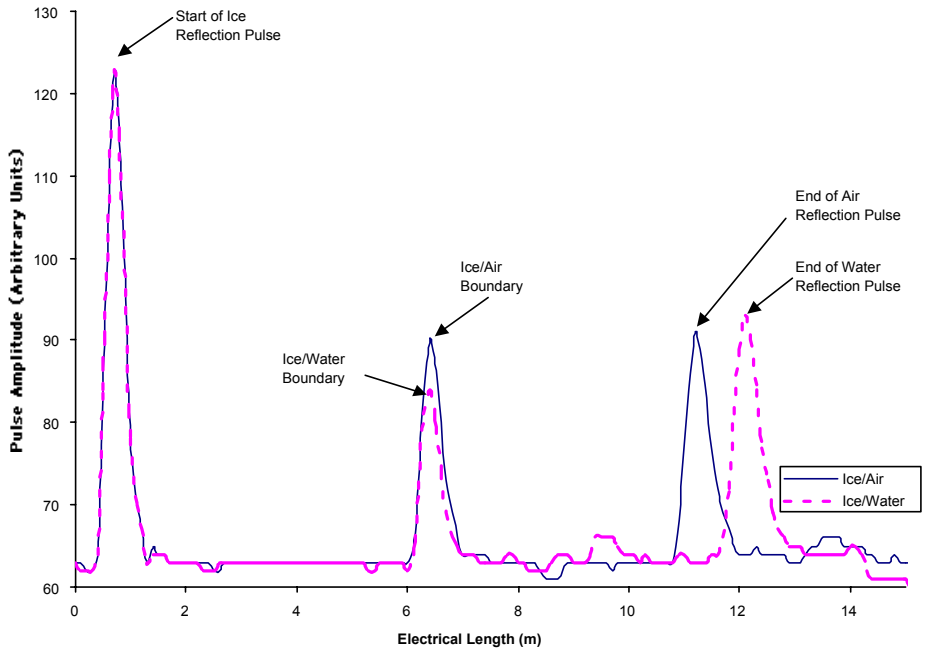

Figure 15. Helicopter blade tests showing TDR waveforms for ice/air and ice/water boundary conditions.

Wing icing tests using TDR

TDR reflection pulse responses were clearly visible at the start-of-sensor, at TDR interconnection between the instrumentation 50-Ω coaxial cable, and the wing-mounted sensor transmission line (Fig. 15). Distinct ice/air and ice/water reflection pulses are also evident along with clearly delineated end-of-sensor reflection pulses. While all expected reflection pulses are clearly visible, the electrical lengths do not agree with what would be expected from a transmission line surrounded by the dielectric materials under test (i.e., air, ice, water). It appears that the effect of the insulation on the sensor wire and the contact with the composite surface of the helicopter blade have a significant overriding effect.

The sensor cable affixed to the helicopter wing was approximately 3 m long. Half of the length, 1.5 m, was covered by a layer of ice. In the ideal situation, a 1.5-m length of transmission line encased in ice with $\varepsilon' = 3.12$ should indicate an electrical length of 2.67 m. Here, we measured an electrical length of approximately 6 m, resulting in a value of $\varepsilon' = 16.0$. Similarly for the air portion of the TDR trace, the physical length of the transmission line exposed to air should exhibit an electrical length of approximately 1.5 m. Here the electrical length is indicated as 4.8 m, translating into an $\varepsilon' = 10.24$. In the case of the TDR waveform with the 1.5-m section covered with water, an electrical length of 5.7 m was observed, translating into an $\varepsilon' = 14.5$. Clearly, the values of the dielectric constant for ice and water as calculated from the known physical length and the measured electrical length of the transmission line sections do not match the known dielectric constants for ice ($\varepsilon' = 3.12$), air ($\varepsilon' = 1$), and water ($\varepsilon' = 80$).

The wire insulation and effects of the underlying composite material structure of the helicopter blade appear to significantly bias the TDR readings. This is supported by the sensitivity measurements as conducted by Baker and Lascano (1989) and Knight (1992). They confirm that a TDR parallel transmission line's greatest sensitivity is directly between, and in immediate proximity to, the two transmission line wires. Sensitivity drops sharply with increasing distance.

Similar results occurred during anti-icing fluid measurements tests. The effect of the dielectric of the sensor wire insulation and the wing's proximity to the sensor was evident. Again, dielectric values as measured with a network analyzer do not agree with values inferred from these TDR tests (Fig. 14 and 15). While the network analyzer indicated dielectric values in the range of approximately 50 to 70, dielectric values in the range of 3 to 5 were calculated from the data shown in Figures 16 and 17. Here, various concentration solutions of deicing and anti-icing fluids were permitted to gradually warm to room temperature (~25°C) after having cold-soaked for several hours at –10°C. A slight

change in electrical length is seen in all cases as the glycol solutions warm over a time period of three hours.

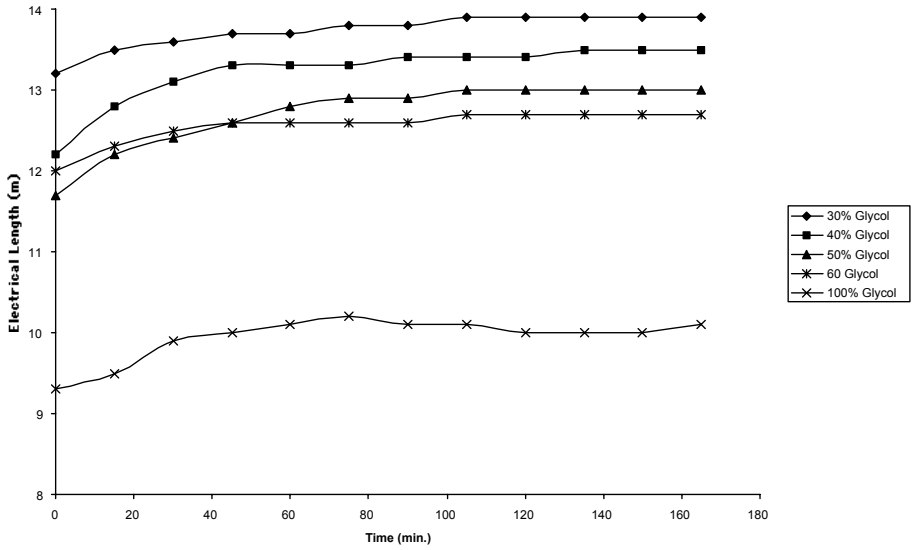

Figure 16. Electrical length vs. time for warming of several concentrations of a glycol-based deicing solution applied to a 3-m section of Black Hawk helicopter rotor blade.

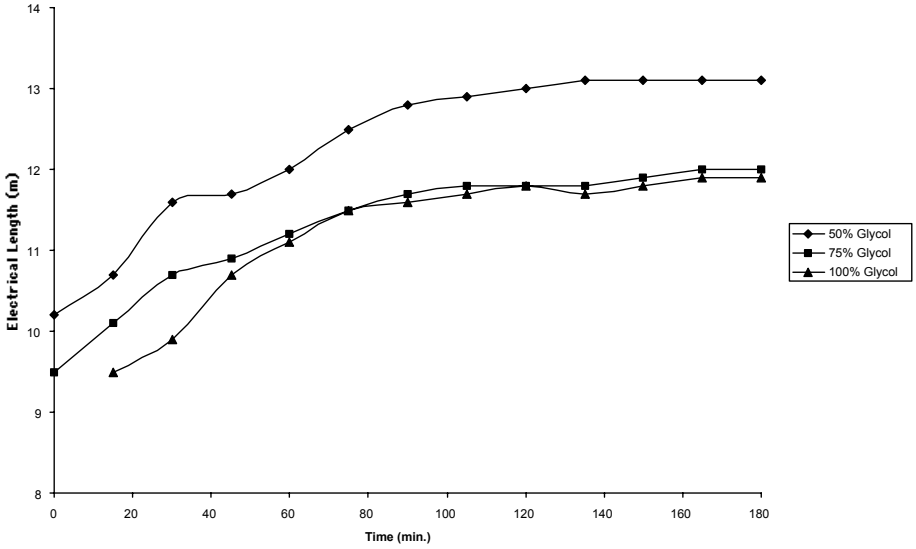

Figure 17. Electrical length vs. time for warming of several concentrations of a glycol-based anti-icing solution applied to a 3-m section of Black Hawk helicopter rotor blade.

4 CONCLUSIONS

The boundary between ice and air or ice and water was distinct and discernable in the TDR traces.

The boundaries between ice and an adjacent deicing (or anti-icing) solution were less distinct and difficult to discern with the TDR. We speculate that this was most likely due to the action of the deicer creating a mixed phase zone (varying solution of ice, water, and deicer), a dielectric gradient at the boundary.

In a laboratory environment we were able to detect single air/ice, water/ice, and glycol/ice interfaces along relatively short (1- to 2-m-) structures. However, because of the high electrical loss of glycol-based deicers and the potential complexity of ice formations (with a multiplicity of phase and solution boundaries) on long (several meters to tens of meters) wing/blade structures in a natural environment, TDR as configured in these experiments may be impractical for operational use.

The lower electrical losses exhibited by water (relative to those of glycol solutions) would not as greatly inhibit the use of TDR in ice/water boundary detection on longer sensor elements than used in the laboratory. However, in natural environments, the spatial variability and physical scale of multiple adjacent phase boundaries (air/ice, water/ice, etc.) will most likely be spatially random and frequently scaled below the resolution capability of a practically implementable TDR pulse width. If the variability is below pulse width spatial scale, then it would be difficult to decipher TDR waveforms and spatial boundary conditions.

While the resolution of multiple and closely spaced boundary transitions may be difficult to resolve with TDR, a pulse-based transmission line system, either based on TDR or on transmitted/reflected power, may have potential to determine the bulk or integrated dry/wet/iced/deicing or anti-icing fluid state of an aircraft wing, rotor, or airframe component.

In both the trough- and tube-based tests, the TDR sensor transmission line conductors were bare (uninsulated) wires that were fully suspended in either air, water, or an anti-icing or deicing solution. Here, the effect of the dielectric materials under test were fully experienced by the sensor. For the helicopter blade-mounted tests the TDR sensor transmission line was fabricated from an insulated “ribbon cable” pair and affixed directly to the blade surface. We believe that both the wire insulation and the contact with the helicopter blade affected the ability of the TDR to accurately sense and measure the dielectric of the overlying ice, water, or glycol solutions. The wire insulation, a dielectric material, partially

filled the volume of sensitivity as defined in equation 7. Similarly, the sensor wires in contact with the helicopter blade permitted only half of the cylindrical volume around the sensor wires to come in contact with the ice, water, or glycol solutions. The other half-cylindrical portion of the volume was affected by the dielectric properties of the composite wing structure. This configuration modified the bulk dielectric measured and the sensitivity of the TDR to changes in the dielectric of the overlying ice, water, or dielectric solutions. This is supported by the sensitivity measurements as conducted by Baker and Lascano (1989) and Knight (1992). A more effective wing surface TDR wire sensor would be helpful for any future experiments. Appropriate modifications to the sensor would increase the exposure of the parallel transmission line to the surrounding air, water, ice, and glycol environment and would minimize the effects of other adjacent dielectric materials.

5 FUTURE WORK

We are continuing to explore and refine the use of electromagnetic and optical techniques to obtain in-situ or contact-based (as opposed to remotely sensed) bulk (integrated) and spatial indication of wing icing conditions.

LITERATURE CITED

Baker, J.M., and R.J. Lascano (1989) The spatial sensitivity of time domain reflectometry. *Soil Science*, **147**(5): 378–384.

Botros, A.Z., and A.D. Oliver (1986) Analysis of target response of FM–CW radar. *IEEE Transactions on Antennas and Propagation*, Vol. AP-34, No. 4, 575–581.

Botros, A.Z., and A.D. Oliver (1986) Analysis of target response of FM-CW radar. IEEE Transactions on Antennas and Propagation, Vol. AP-34, No. 4, 575–581.

Duncan, P. (1995a) The clean aircraft concept, Part 1. *FAA Aviation News*, Vol. 34, No. 7: 3–6.

Duncan, P. (1995b) The clean aircraft concept, Part 2. *FAA Aviation News*, Vol. 34, No. 8: 1–4.

Duncan, P. (1996) The clean aircraft concept, Part 3. *FAA Aviation News*, Vol. 35, No. 1: 1–5.

FAA (1994) Ground Deicing and Anti-Icing Training and Checking. Federal Aviation Administration Advisory Circular 135-16, AFS-250, 12 December 1994.

Knight, J.H. (1992) Sensitivity of time domain reflectometry measurements to lateral variations in soil water content. *Water Resources Research*, **28**(9): 2345–2352.

NTSB (1996) In-flight icing encounter and loss of control, Simmons Airlines, d.b.a. American Eagle Flight 4184, Avions de Transport Regional (ATR) Model 72-212, N401AM, Roselawn, Indiana, 31 October 1994. Aircraft Accident Report NTSB/AAR-96/01, Volume 1: Safety Board Report.

NTSB (1997) In-flight icing encounter and uncontrolled collision with terrain, Comair Flight 3272, Embraer EMB-120T, N265CA, Monroe, Michigan, 9 January 1997. Aircraft Accident Report NTSB/AAR-98/04.

Ray, P.S. (1972) Broadband complex refractive indices of ice and water. *Applied Optics*, **11**(8):1836–1843.

SAE (1995) Aircraft Ice Detectors and Icing Rate Measuring Instruments. Society of Automotive Engineers, Aviation Information Report 4367, April 1995, AC-9C, Aircraft Icing Technology Subcommittee.

SAE (2001) Minimum Operational Performance Specification for Inflight Icing Detection Systems. Society of Automotive Engineers, Aviation Specification 5498, October 2001.

Skolnick, M.L. (1980) *Introduction to Radar Systems*. New York: McGraw–Hill, 581 p.

Stove, A.G. (1992) Linear FMCW radar techniques. *IEEE Proceedings*, Vol. 139, No. 5, 343–350.

Ulaby, F.T., R.K. Moore, and A.K. Fung (1986) Microwave Remote Sensing—Active and Passive. Norwood, Massachusetts: Artech House, Inc.

Yankielun, N.E. (2001) Transmission Line Reflectometer Using Frequency Modulated–Continuous Wave. U.S. Patent 6,281,688.

Yankielun, N.E., S.A. Arcone, and R.K. Crane (1992) Thickness profiling of freshwater ice using a millimeter-wave FM–CW radar. *IEEE Transactions on Geoscience and Remote Sensing*, **30**: 1094–1100.

REPORT DOCUMENTATION PAGE

Form Approved
OMB No. 0704-0188

1. REPORT DATE *(DD-MM-YY)*	2. REPORT TYPE	3. DATES COVERED *(From - To)*
October 2002	Technical Report	

4. TITLE AND SUBTITLE

Wide-Area Ice Detection Using Time Domain Reflectometry

5a. CONTRACT NUMBER

5b. GRANT NUMBER

5c. PROGRAM ELEMENT NUMBER

6. AUTHOR(S)

Norbert E. Yankielun, Charles C. Ryerson, and Sarah L. Jones

5d. PROJECT NUMBER

5e. TASK NUMBER

5f. WORK UNIT NUMBER

7. PERFORMING ORGANIZATION NAME(S) AND ADDRESS(ES)

U.S. Army Engineer Research and Development Center
Cold Regions Research and Engineering Laboratory
72 Lyme Road
Hanover, NH 03755-1290

8. PERFORMING ORGANIZATION REPORT NUMBER

ERDC/CRREL TR-02-15

9. SPONSORING/MONITORING AGENCY NAME(S) AND ADDRESS(ES)

Office of the Chief of Engineers
Washington, DC

10. SPONSOR / MONITOR'S ACRONYM(S)

11. SPONSOR / MONITOR'S REPORT NUMBER(S)

12. DISTRIBUTION / AVAILABILITY STATEMENT

Approved for public release; distribution is unlimited.

Available from NTIS, Springfield, Virginia 22161.

13. SUPPLEMENTARY NOTES

14. ABSTRACT

Ice accretion on the wings of fixed-wing aircraft and on the rotors of rotary-wing aircraft can have disastrous results. The ice that forms on a wing structure, especially along the leading edge, modifies the wing aerodynamics, resulting in decreased lift. In the extreme, this can lead to stall and loss of control of the aircraft and potentially a crash. Ice building up elsewhere on the wing, rotor, or airframe can add weight to the aircraft. Several techniques and flight protocols have been developed and are widely used to prevent aircraft from becoming ice covered, both in flight and on the ground.

15. SUBJECT TERMS

Aircraft, Anti-icing fluid, Deicing, Deicing fluid, Glycol, Ice, Icing, TDR, Time domain reflectometry

16. SECURITY CLASSIFICATION OF:			17. LIMITATION OF ABSTRACT	18. NUMBER OF PAGES	19a. NAME OF RESPONSIBLE PERSON
a. REPORT	b. ABSTRACT	c. THIS PAGE			19b. TELEPHONE NUMBER *(include area code)*
U	U	U	U	37	

DEPARTMENT OF THE ARMY
ENGINEER RESEARCH AND DEVELOPMENT CENTER, CORPS OF ENGINEERS
COLD REGIONS RESEARCH AND ENGINEERING LABORATORY, 72 LYME ROAD
HANOVER, NEW HAMPSHIRE 03755-1290

Official Business